PHYSICAL REVIEW D

PARTICLES AND FIELDS

THIRD SERIES, VOL. 3, NO. 3 1 FEBRUARY 1971

Coherent Production of Pions in Deuterium at 5.4 GeV/c*

B. J. DEERY,† N. N. BISWAS, N. M. CASON, T. H. GROVES,‡ P. B. JOHNSON,§ V. P. KENNEY, J. A. POIRIER, O. A. SANDER, P. H. SMITH, AND W. D. SHEPHARD

Department of Physics, University of Notre Dame, Notre Dame, Indiana 46556

(Received 18 August 1970)

The reaction $\pi^+d \to d\pi^+\pi^+\pi^-$ has been investigated at an incident pion beam momentum of 5.4 GeV/c. The three-pion system is observed to be coherently produced off the deuteron target. The reaction is dominated by the quasi-three-body final state $d\rho^0\pi^+$. D^* enhancements are observed, but they appear to be the result of kinematic reflections from the $d\rho^0\pi^+$ system. The striking feature of this reaction is the presence of a broad, structureless, low-mass three-pion enhancement in the region between 0.9 and 1.5 GeV.

I. INTRODUCTION

IN this paper we study the reaction

$$\pi^+d \to d\pi^+\pi^+\pi^- \qquad (1)$$

at an incident pion beam momentum of 5.4 GeV/c. We find that the three-pion system is peripherally produced off the deuteron target; this low four-momentum transfer to the target is characteristic of the coherent interaction of the pion beam with the target deuteron as a whole. We observe that reaction (1) is dominated by the quasi-three-body final state

$$\pi^+d \to d\rho^0\pi^+. \qquad (1')$$

This result is consistent with that of other experiments[1–7] for $\pi^\pm d$ interactions in the pion momentum range 2.7–8.0 GeV/c. The presence of the previously reported D^{*++} and D^{*0} enhancements is observed in this experiment. However, these enhancements are shown to be the kinematic consequence of the peripheral production of the ρ^0 in reaction (1′). A broad low-mass enhancement in the three-pion mass distribution is observed as a characteristic feature of reaction (1).

A spin-parity analysis has been applied to the data in the region of the broad diffractive enhancement, $0.9 \leq M(3\pi) \leq 1.5$ GeV. We find the data to be consistent with a $J^P = 1^+$ spin-parity state. The dynamics of this coherently produced low-mass 3π system can be understood in terms of the Veneziano model.[8,9]

II. EXPERIMENTAL PROCEDURE

The data used for this analysis were obtained from two separate runs in the Argonne National Laboratory ZGS 7° beam. The deuterium-filled MURA 30-in. bubble chamber was exposed to an electrostatically separated π^+ beam of 5.4 GeV/c incident momentum. The two runs yielded approximately 140 000 four-view photographs of the chamber containing an average of 13.1 beam tracks per picture.

The film was scanned for all four-prong events within a defined fiducial volume. An independent second scan

* Research supported in part by the National Science Foundation.

† Present address: University of Nijmegen, Nijmegen, Holland. This work was done in partial fulfillment of the requirements for the degree of Doctor of Philosophy of the University of Notre Dame.

‡ Present address: Argonne National Laboratory, Argonne, Ill. 60439.

§ Present address: IBM, Owego, New York.

[1] L. Seidlitz, O. I. Dahl, and H. D. Miller, in *Proceedings of the Athens Second Topical Conference on Resonant Particles, 1965*, edited by B. A. Munir (Ohio U. P., Athens, Ohio, 1965), p. 162.

[2] M. A. Abolins, D. D. Carmony, R. L. Lander, and Ng.-h. Xuong, Phys. Rev. Letters **15**, 125 (1965).

[3] A. Forino, R. Gessaroli, L. Lendinara, G. Quareni, A. Quareni-Vignudelli, M. Armenise, B. Ghidini, V. Picciarelli, A. Romano, A. Cartacci, M. G. Dagliana, M. Della Corte, G. Dicaporiaco, J. Laberrigue-Frolow, Nguyen Huu Khanh, J. Quinquart, M. Sené, W. Fickinger, and O. Goussu, Phys. Letters **19**, 68 (1965).

[4] D. Avison, J. Campbell, C. Ezell, A. F. Garfinkel, J. Gezelter, S. Lichtman, F. Loeffler, R. Miller, and P. Willman, in *Proceedings of the Fourteenth International Conference on High-Energy Physics, Vienna, 1968*, edited by J. Prentki and J. Steinberger (CERN, Geneva, 1968).

[5] G. Vegni, H. Winzeler, P. Zaniol, P. Fleury, and G. DeRosny, Phys. Letters **19**, 562 (1965).

[6] A. M. Cnops, P. V. C. Hough, F. R. Huson, I. R. Kenyon, J. M. Scarr, I. O. Skillicorn, H. O. Cohn, R. D. McCulloch, W. M. Bugg, G. T. Condo, and M. N. Nussbaum, Phys. Rev. Letters **21**, 1609 (1968).

[7] B. Eisenstein and H. Gordon, Phys. Rev. D **1**, 841 (1970).

[8] G. Veneziano, Nuovo Cimento **57A**, 190 (1968).

[9] B. J. Deery, J. E. Mansfield, N. N. Biswas, N. M. Cason, V. P. Kenney, J. A. Poirier, and W. D. Shephard, Phys. Letters **31B**, 82 (1970).

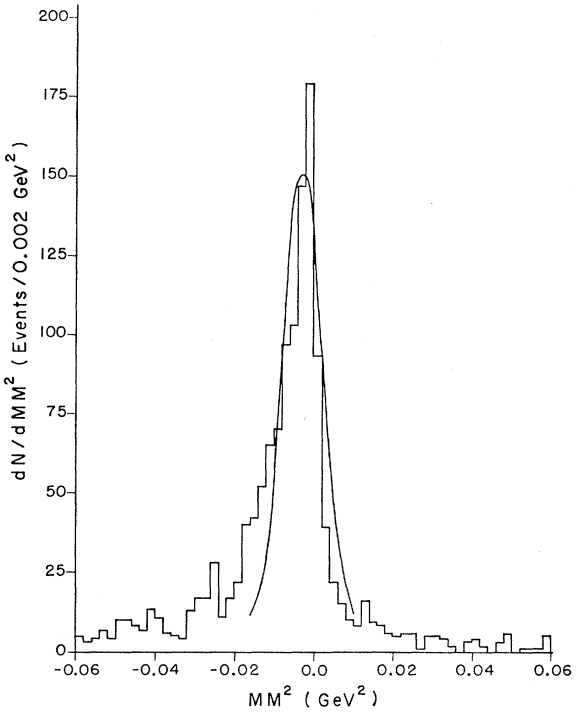

FIG. 1. Distribution of the square of the missing mass for the 1414 events which obtained a GRIND fit to reaction (1). Solid line represents a hand-drawn Gaussian curve centered at $MM^2 = -0.003$ GeV^2 with a standard deviation of 0.06 GeV^2.

was completed on segments of the whole experiment to obtain estimates of event loss and of single-scan efficiency. We required at least one outgoing track to stop in the chamber, which accounted for approximately 40% of the 72 000 four-prong events. The measurements were then processed through the geometry reconstruction program HAG (the Notre Dame version of HGEOM) and the kinematic fitting program GRIND. The events were fitted to the following reaction hypotheses:

$$\pi^+ d \rightarrow d\pi^+\pi^+\pi^- \quad (1)$$

$$\rightarrow pn\pi^+\pi^+\pi^- \quad (2)$$

$$\rightarrow pp\pi^+\pi^-, \quad (3)$$

and the corresponding reactions with additional neutral pions. Events which fit reaction (1) were reexamined to ascertain whether or not the track ionizations predicted from fitted momenta were consistent with the event.

A total of 1414 events fitted reaction (1). The missing-mass-squared distribution for these events is shown in Fig. 1. We required $-0.02 \leq MM^2 \leq 0.02$ GeV^2 to reduce the contamination of events with π^0 production and of badly measured events. Of the sample of 1043 events which remained after the missing-mass cut, 364 events were found to give unique fits to reaction (1). The remaining 679 events were ambiguous between reactions (1) and (2). There were no ambiguities between reactions (1) and (3).

Most events which gave fits to reaction (1) had one track stopping in the chamber. The ionization of this track frequently was consistent with both proton and deuteron mass assignments. For a given stopping-track length, the ratio of the momentum of an assumed proton to the momentum of an assumed deuteron is

$$|\mathbf{p}_p|/|\mathbf{p}_d| \approx \tfrac{3}{5}.$$

Hence, an event of reaction (1) when fitted to reaction (2) would yield a neutron momentum,

$$|\mathbf{p}_n| \approx \tfrac{2}{3}|\mathbf{p}_p|.$$

Further, the fitting of reaction (2) to events of reaction (1) will tend to make the neutron and proton momentum collinear, i.e., $\cos\theta(\mathbf{p}\cdot\mathbf{n}) \approx 1$. A scattergram of $\cos\theta(\mathbf{p}\cdot\mathbf{n})$ versus the ratio of the fitted nucleon momenta from fits to reaction (2) was used to study the 679 ambiguous events, as shown in Fig. 2. The concentration of events in the predicted correlation region indicates that most of the ambiguous events belong to reaction (1). From Fig. 2 we required $0.4 \leq |\mathbf{p}_n|/|\mathbf{p}_p| \leq 1.2$ and $\cos\theta(\mathbf{p}\cdot\mathbf{n}) \geq 0.4$, with the result that 528 events were classified with reaction (1). A χ^2-probability cut of $\geq 2\%$ in the GRIND kinematic fit was imposed, leaving a final sample of 793 events for reaction (1).

III. PROPERTIES OF REACTION

The highly peripheral nature of the interaction is indicated in Fig. 3, which shows the distribution of t, the square of the four-momentum transfer between the initial- and final-state deuterons. A maximum-likelihood

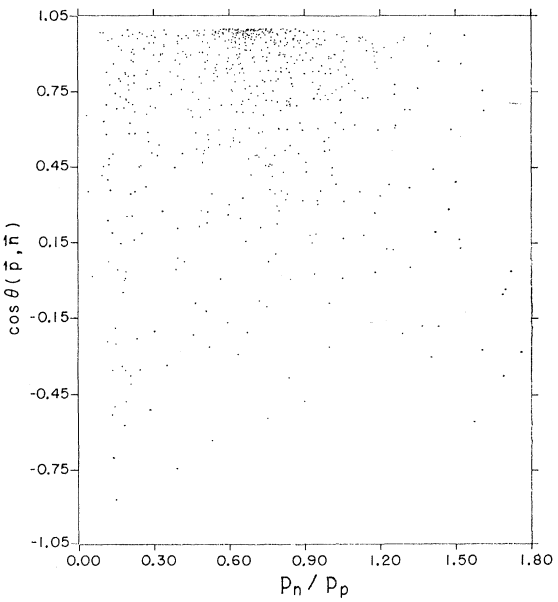

FIG. 2. Scattergram for $\cos\theta(p,n)$, the laboratory angle between the neutron and protron, versus $|\mathbf{p}_n|/|\mathbf{p}_p|$, the ratio of the magnitudes of the nucleon laboratory momenta, obtained from fits to reaction (2) for the 679 events ambiguous between reactions (1) and (2).

fit to the data using the expression

$$N = N_0 e^{-\alpha|t|} \quad (4)$$

yields $\alpha = 17.2 \pm 1.3$ $(\mathrm{GeV}/c)^{-2}$ in the region $0.04 \leq t \leq 0.08$ $(\mathrm{GeV}/c)^2$. Below $|t| = 0.04$ $(\mathrm{GeV}/c)^2$, there was a systematic loss of events resulting from the deuteron stopping in the chamber without leaving a visible track. The upper limit on $|t|$ was made on the basis of statistics. The curve in Fig. 3 shows the best fit to the data. The steep slope of the t distribution is typical of the coherent interaction of the incident pion with the deuteron target as a whole.

A. Two-Particle Systems

The $\pi^+\pi^-$ effective-mass spectrum is shown in Fig. 4(a); the distribution shows strong ρ^0 production. No f^0 or g^0 meson production is observed; we note that production of high dipion masses is suppressed by the very peripheral nature of the reaction. The accumulation of events just above threshold is a consequence of the fact that whenever one $\pi^+\pi^-$ mass combination forms a ρ^0, the other $\pi^+\pi^-$ combination is constrained to have a low effective mass. The curve represents a three-parameter maximum-likelihood fit with a Breit-Wigner resonance of mass-independent width. Background was estimated using the program FAKE, a Monte Carlo program which generates events accord to relativistic phase space. Background estimates were made separately for the peripheralized nonresonant $d3\pi$ final state

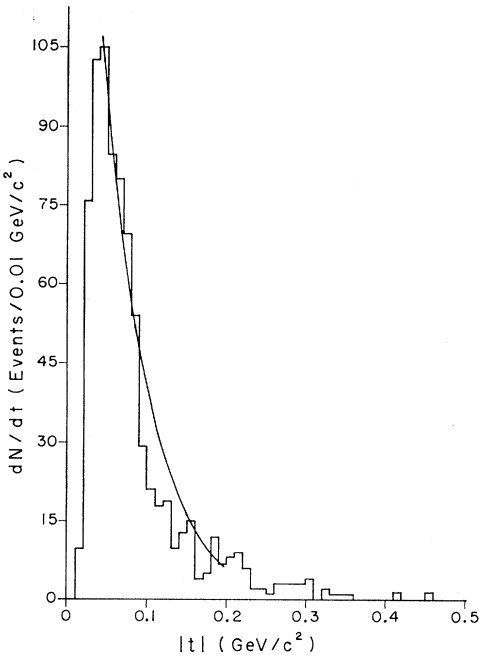

FIG. 3. Distribution of the square of the four-momentum transfer to the deuteron target for the 793 events of reaction (1). The curve represents a maximum-likelihood fit to the data with the peripherality constant $\alpha = 17.2$ $(\mathrm{GeV}/c)^{-2}$ for the region $0.04 \leq |t| \leq 0.08$ (GeV/c^2).

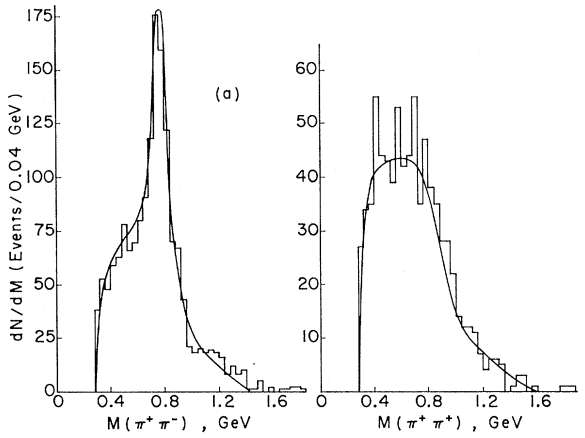

FIG. 4. (a) $\pi^+\pi^-$ effective-mass distribution for the 793 events of reaction (1), with one entry for each of two possible neutral dipion pairings per event. The curve represents a three-parameter maximum-likelihood fit using a single Breit-Wigner form to describe the resonance, as described in the text. (b) $\pi^+\pi^+$ effective-mass distribution for the same events. The curve is the Monte Carlo estimate of background.

B_{PS}, and for the ρ^0 reflection in a peripheralized final state $d\rho^0\pi^+$ B_{ref}. The Breit-Wigner resonance factor K_{BW} was combined with the background terms in the expression

$$dN/dM = 2(1-P)B_{\mathrm{PS}} + P(K_{\mathrm{BW}}B_{\mathrm{PS}} + B_{\mathrm{ref}}), \quad (5)$$

where P is the fraction of ρ^0 production. Using the maximum-likelihood method, we obtain the mass $M(\rho)$, the width $\Gamma(\rho)$, and P as $M(\rho) = 0.772 \pm 0.005$ GeV, $\Gamma(\rho) = 0.130 \pm 0.012$ GeV, and $P(\rho) = 0.75 \pm 0.05$.

The $\pi^+\pi^+$ effective-mass spectrum for the same events is shown in Fig. 4(b). The distribution shows no evidence of any $I = 2$ resonant structure. The curve represents the distribution of the FAKE-generated events described above.

The π^-d and π^+d effective-mass distributions are shown in Figs. 5(a) and 5(b). The D^{*0} enhancement previously reported[1–6] in the low π^-d mass region is observed, but is no longer evident when we require both $\pi^+\pi^-$ mass combinations to be outside the ρ^0 region (shaded). In the π^+d mass distribution, the D^{*++} enhancement is prominent. If we assumed that the distribution of Fig. 5(b) was due to a D^{*++} resonance and a background composed of a peripheralized, nonresonant $d3\pi$ final state and reflection from the $D^{*++}\pi^+\pi^-$ final state, we would obtain the values $M(D^*) = 2.179 \pm 0.012$ GeV and $\Gamma(D^*) = 0.270 \pm 0.024$ GeV. The fractional amount of D^* would be $P(D^*) = 0.54 \pm 0.03$. These values are obtained using an expression of the form (5).

Arguments can be presented against a resonance interpretation of the D^{*++} enhancement. The D^{*++} c.m. decay angle distribution is shown in Fig. 5(c) for events with $2.0 \leq M(\pi^+d) \leq 2.4$ GeV. [If an event had both π^+d mass combinations in the D^{*++} region, the π^+d mass combination closer to the D^{*++} value, $M(D^*)$

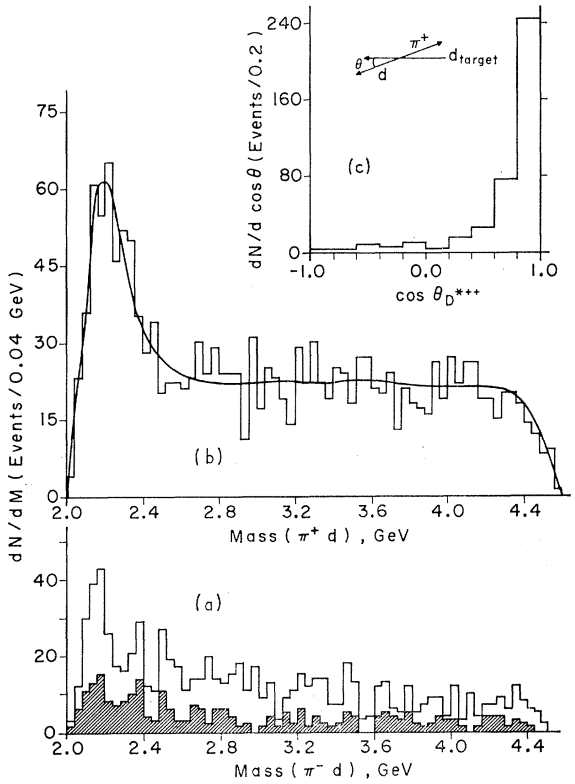

FIG. 5. (a) $\pi^- d$ effective-mass distribution for events of reaction (1). The shaded events have $0.66 \leq M(\pi^+\pi^-) \leq 0.86$ GeV. (b) $\pi^+ d$ effective-mass distribution. The curve represents a three-parameter maximum-likelihood fit to the data. (c) c.m. decay-angle distribution of the $\pi^+ d$ system in the D^{*++} region, $2.0 \leq M(\pi^+ d) \leq 2.4$ GeV, where θ_{D^*} is defined as the angle between the outgoing deuteron from the D^{*++} decay and the deuteron target in the D^{*++} c.m. system.

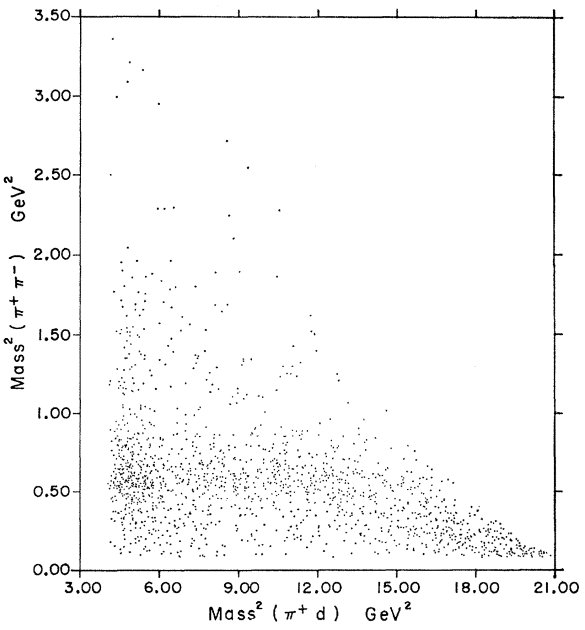

FIG. 6. Scattergram of the square of the $\pi_1^+\pi^-$ effective mass versus the square of the effective mass of the (other) $\pi_2^+ d$ (two entries per event).

$= 2.179$ GeV, was chosen.] The distribution is very asymmetric, with events concentrating at $\cos\theta \geq 0.6$. Even considering possible interference effects, it is most unlikely that a D^* resonance with such low mass would decay so asymmetrically.

In Fig. 6 we show a scatterplot of the square of the $\pi_1^+\pi^-$ effective mass versus the square of the $\pi_2^+ d$ effective mass. Most of the events with $4.0 \leq M^2(\pi^+ d) \leq 5.8$ GeV^2 cluster in the ρ^0 overlap region, indicating strong D^{*++}-ρ correlation. Figure 7 shows the Van Hove plot for the $d\rho^0\pi^+$ final state. An event is represented as a single point whose distances from the three axes are proportional to the c.m. longitudinal momenta of the three final-state particles. As a result of the peripheral character of the interaction, the longitudinal momentum of the deuteron is strongly negative and concentrated near the kinematic limit. The longitudinal momentum of the ρ^0 is almost always in the forward (positive) direction. When the ρ^0 is produced with high positive longitudinal momentum, both the other π^+ and the deuteron generally have negative longitudinal momenta, and a $\pi^+ d$ enhancement at low mass (the D^{*++}) results from the kinematics. Since the observed enhancement can be understood as a consequence of the $d\rho^0\pi^+$ final state, a resonance interpretation is unnecessary. Total and partial cross sections for reaction (1) are summarized in Table I.

B. Three-Pion System

The three-pion effective-mass distribution is shown in Fig. 8. We note that this distribution is derived from the

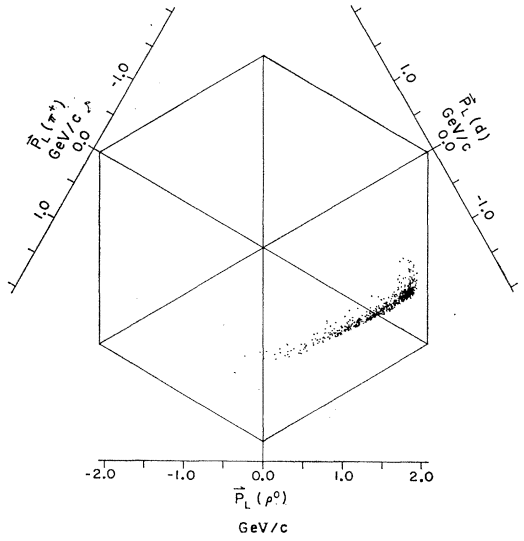

FIG. 7. Van Hove plot for the $d\rho^0\pi^+$ final state, where the ρ^0 was selected by requiring $0.64 \leq M(\pi^+\pi^-) \leq 0.88$ GeV. If both $\pi^+\pi^-$ combinations were in this interval, the combination having the smaller value of Δ^2 (the square of the four-momentum transfer from the beam to the $\pi^+\pi^-$ system) was chosen. Each event is represented by a single point whose distances from the three axes are proportional to the c.m. longitudinal momenta of the three final-state particles.

TABLE I. Cross sections.

Reaction	Cross section (μb)
$\pi^+d \rightarrow d\pi^+\pi^+\pi^-$ (total)	408±80
$\rightarrow d\pi^+\pi^+\pi^-$ (nonres.)	102±25
$\rightarrow d\rho^0\pi^+$	306±75

measurements of four-prong events and does not include events with very low four-momentum transfer between the incident and the outgoing deuteron (the three-prong events). From the study of the Chew-Low plot of $M(3\pi)$ versus momentum transfer, we find that the three-prong events would influence the mass spectra for $M(3\pi)\leq 1.35$ GeV. Using events generated by a Monte Carlo method corresponding to the $d\rho\pi^+$ final state, we estimate the loss of events due to low four-momentum transfer to be (20.3±5)%. This correction has been taken into account for the cross sections shown in Table I, but not in the mass distribution shown in Fig. 8.

The mass distribution is characterized by a broad low-mass enhancement in the mass region $0.9\leq M(3\pi)\leq 1.5$ GeV. We note that this broad mass enhancement includes the $A_1(1080)$ and $A_2(1300)$ regions, although we observe no significant peaking at the nominal mass values. The depletion of events in the low three-pion mass region, $M(3\pi)<0.8$ GeV, was found to be due to the dominance of the $d\rho^0\pi^+$ final state; the minimum three-pion effective mass is constrained to be greater than ~0.9 GeV.

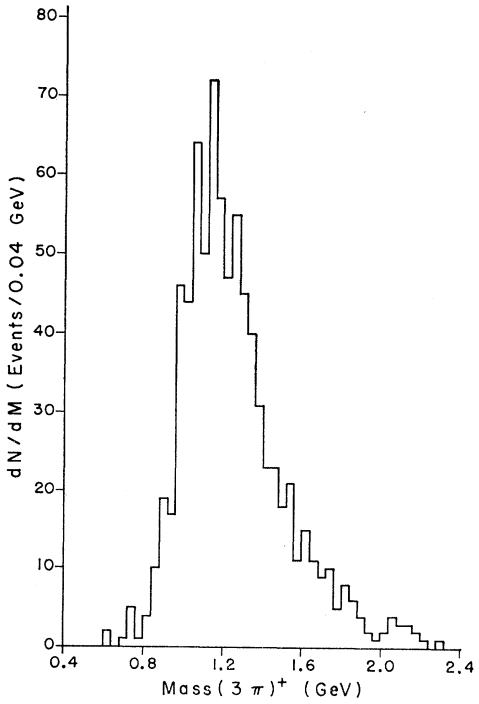

FIG. 8. $\pi^+\pi^+\pi^-$ effective-mass distribution for the events of reaction (1).

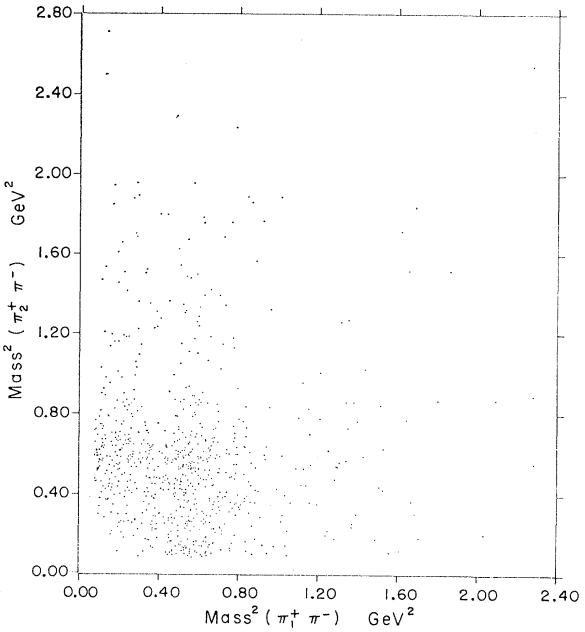

FIG. 9. Dalitz plot $M^2(\pi_1^+\pi^-)$ versus $M^2(\pi_2^+\pi^-)$ for the 3π system of reaction (1) (two points per event).

The Dalitz plot for events with $0.9\leq M(3\pi)\leq 1.5$ GeV is shown in Fig. 9. The prominence of the ρ^0 bands is evident.

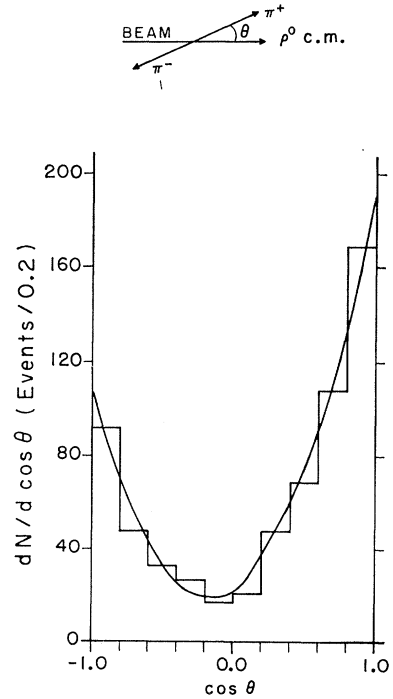

FIG. 10. Decay-angle distribution of the ρ^0 for events with $0.9\leq M(3\pi)\leq 1.5$ GeV. The angle θ is the angle between the outgoing π^+ and the beam direction in the ρ^0 rest frame. The curve represents a maximum-likelihood fit to the distribution considering s- and p-wave interference in the dipion system.

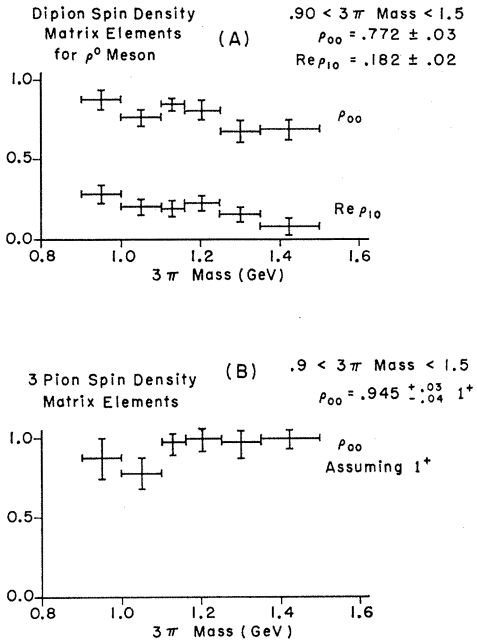

FIG. 11. (a) Two-pion spin-density matrix elements ρ_{00} and $\mathrm{Re}\rho_{10}$ for ρ^0 decay as a function of three-pion effective mass. (b) Three-pion spin-density matrix element ρ_{00} for the decay of the 3π system, assuming $J^P=1^+$, as a function of 3π mass.

IV. ANALYSIS OF 3π ENHANCEMENT

A. Spin-Density Matrix Elements for $\pi^+\pi^-$ System

Since ρ^0 production dominates reaction (1), we analyzed the ρ^0 decay angle distribution as a function of $M(3\pi)$ for events with $0.9\leq M(3\pi)\leq 1.5$ GeV. Figure 10 shows the ρ^0 decay angle distribution for all events in this mass interval, where θ is the angle between the outgoing π^+ and the beam direction in the ρ^0 rest frame. The curve represents the best fit to the distribution for the expression

$$dN/d\cos\theta=\tfrac{3}{4}[(1-\rho_{00})+(3\rho_{00}-1)\cos^2\theta]+\sqrt{3}\,\mathrm{Re}\rho_{10}\cos\theta.$$

Only s- and p-wave $\pi\pi$ interactions are included; the element $\mathrm{Re}\rho_{10}$ is due to s- and p-wave interference.

TABLE II. ρ^0 decay angular distribution.

3π mass (GeV)	Events	Density-matrix element ρ_{00}	Density-matrix element $\mathrm{Re}\rho_{10}$	χ^2 CL[a] (%)
0.90–1.00	71	$0.881_{-0.066}{}^{+0.055}$	$0.281_{-0.058}{}^{+0.057}$	33
1.00–1.10	132	$0.776_{-0.053}{}^{+0.051}$	$0.199_{-0.050}{}^{+0.043}$	45
1.10–1.18	124	$0.853_{-0.057}{}^{+0.046}$	$0.195_{-0.048}{}^{+0.045}$	95
1.18–1.25	88	$0.816_{-0.069}{}^{+0.062}$	$0.229_{-0.056}{}^{+0.052}$	95
1.25–1.35	119	$0.675_{-0.067}{}^{+0.069}$	$0.160_{-0.049}{}^{+0.047}$	92
1.35–1.50	98	$0.693_{-0.069}{}^{+0.065}$	$0.086_{-0.057}{}^{+0.057}$	55
0.9 –1.50	632	$0.772_{-0.062}{}^{+0.025}$	$0.182_{-0.021}{}^{+0.021}$	80

[a] Confidence level.

The values of ρ_{00} and $\mathrm{Re}\rho_{10}$, determined by maximum-likelihood analysis, are shown as a function of 3π mass in Fig. 11(a). The strong transverse alignment of the ρ^0 with respect to the beam, indicated by the large values of ρ_{00}, is evident at all values of the 3π mass. The interference between the s- and p-wave contributions in the decay, as indicated by $\mathrm{Re}\rho_{10}$, is appreciable at low 3π mass and shows some tendency to decrease with increasing mass. The values for these density-matrix elements for different mass values, computed by the maximum-likelihood method,[10] are summarized in Table II.

B. Spin-Density Matrix Elements of Three-Pion System

We have investigated the spin-parity of the 3π system using the method of Berman and Jacob,[11] which involved the distribution of the angle α between the incident π^+ and the normal to the decay plane in the 3π rest system, shown in Fig. 12. We consider J^P assignments 0^-, 1^+, and 2^-. The natural-parity series 0^+, 1^-, 2^+, ... may be ruled out, since the Clebsch-Gordan coefficients coupling the natural-parity series with a transverse-aligned ρ^0 (noted above) and a pion vanish.

The 0^- assumption leads to an isotropic distribution of $\cos\alpha$, which is inconsistent with the data of Fig. 12.

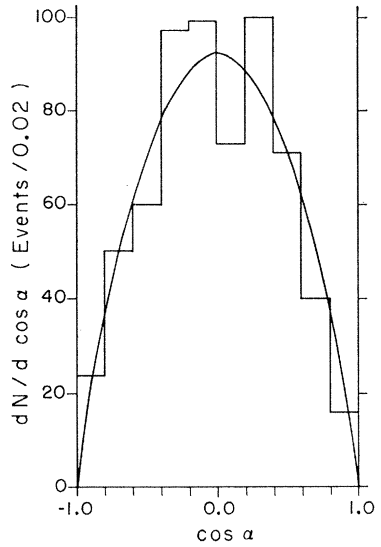

FIG. 12. Distribution of the cosine of the Berman-Jacob angle α for events with $0.9\leq M(3\pi)\leq 1.5$ GeV. Here α is the angle between the normal to the 3π plane and the beam direction in the rest frame of the 3π system. The curve is the maximum-likelihood fit for a pure $J^P=1^+$ state.

[10] We have used the moment method [N. Schmitz, in Proceedings of the 1965 Easter School for Physicists, CERN Report No. 65-24, 1965, Vol. I (unpublished)] to determine the density-matrix elements from the averages of appropriate experimental quantities. The values thus obtained have been utilized in the maximum-likelihood method as initial values which are then allowed to vary to reach the maximum value of the likelihood function. We find than none of the values of the density-matrix elements determined from these two different methods differs significantly.

[11] S. M. Berman and M. Jacob, Phys. Rev. 139, B1023 (1965).

For the 1^+ assumption, the angular distribution is given in terms of the 3π density-matrix element ρ_{00} by

$$dN/d\cos\alpha=\tfrac{3}{4}[(1-\rho_{00})-\tfrac{1}{2}(1-3\rho_{00})\sin^2\alpha].$$

The maximum-likelihood fit shown in Fig. 12 yields the value $\rho_{00}=0.95_{-0.04}{}^{+0.03}$. The fitted values of ρ_{00} for the 3π system are shown as a function of 3π mass in Fig. 11(b). For the 2^- assumption, the maximum-likelihood value of the 3π matrix element ρ_{00} is $0.57_{-0.09}{}^{+0.10}$. When a 3π system decays, the transverse alignment of the resultant dipion will be retained only if no depolarization takes place; if depolarization occurs, the dipion will be less transversely polarized than the 3π system. Thus the transverse alignment of the parent 3π system is expected to be equal to or greater than that of the 2π system. The transverse alignment of the 3π system given for the $J^P=1^+$ assumption is greater than that of the 2π system (Table II), as expected. The fact that the transverse alignment calculated for the 3π system with $J^P=2^-$ would be less than that of the dipion suggests that the $J^P=2^-$ contribution does not dominate.

We have also fitted the angular distributions to a series of Legendre polynominals given by

$$dN/d\cos\alpha=A_0P_0+A_2P_2+A_4P_4.$$

The coefficients A_0, A_2, and A_4 are shown in Fig. 13 as a function of 3π mass. The value of A_4 is consistent with zero within 2 standard deviations for the entire mass region, suggesting that there is no significant contribution from states with $J\geq 2$.

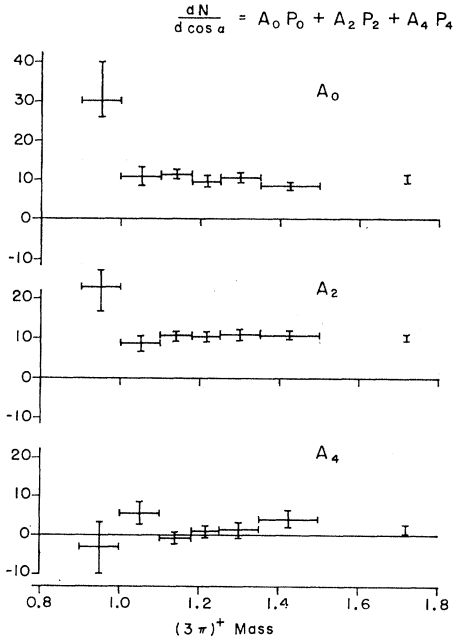

FIG. 13. Best-fit values of coefficients to the Legendre polynomials up to $P_4(\cos\alpha)$. The results are shown for maximum-likelihood fits to each of the mass intervals shown.

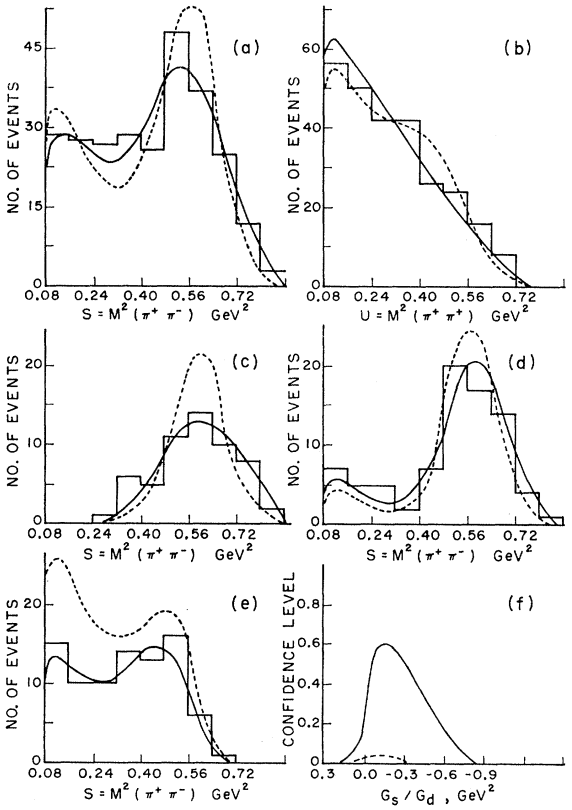

FIG. 14. Projections of the (folded) Dalitz plot of Fig. 9 for events with $1.0\leq M(3\pi)\leq 1.1$ GeV; the nominal A_1 regions are shown in (a)–(e): (a) distribution of $M^2(\pi^+\pi^-)$; (b) distribution of $M^2(\pi^+\pi^+)$; (c) distribution of $M^2(\pi^+\pi^-)$ for $0.08\leq t\leq 0.24$ $(\text{GeV}/c)^2$; (d) distribution of $M^2(\pi^+\pi^-)$ for $0.24\leq t\leq 0.48$ $(\text{GeV}/c)^2$; (e) distribution of $M^2(\pi^+\pi^-)$ for $0.48\leq t\leq 0.72$ $(\text{GeV}/c)^{-2}$; (f) χ^2 confidence level as a function of G_s/G_d. The solid (dashed) curves in these figures correspond to the Veneziano (ρ-pole) model predictions.

C. Application of Veneziano and ρ-Pole Models

We have applied the Veneziano model and a symmetrized ρ-pole model to the three-pion system. Details of the analysis are published elsewhere.[9] For the Veneziano model we take the scattering amplitude $T(\pi^+\pi^-\to\pi^-A_1{}^+)$, where $A_1{}^+$ denotes a pure $J^P=1^+$ 3π state, given by the expression

$$|T|^2=Nb^2F(s,t)\left|\frac{\Gamma(1-\alpha(s))\Gamma(1-\alpha(t))}{\Gamma(2-\alpha(s)-\alpha(t))}\right|^2. \quad (6)$$

Here b is the slope of the ρ-f trajectory, N is an over-all normalization factor, and $F(s,t)$ is a term[9] containing kinematic factors and the parameter G_s/G_d, the ratio of s-wave- and d-wave-related $A_1\rho\pi$ coupling constants. The G_s/G_d ratio is the only free parameter in the analysis. Following Lovelace,[12] we take

$$\alpha(s)=0.483+0.885s+ic(s-4\mu^2)^{1/2}. \quad (7)$$

[12] C. Lovelace, Phys. Letters **28B**, 264 (1968). As suggested by Lovelace, we take the parameter c in expression (7) to be 0.28, which corresponds to an effective width for both ρ-f parent and e^0 daughter trajectories of 294 MeV.

For the conventional ρ-pole model we take the scattering amplitude given by

$$|T|^2 = NF(s,t)\left|\frac{1}{(s-m_\rho^2)+im_\rho\Gamma}+\frac{1}{(t-m_\rho^2)+im_\rho\Gamma}\right|^2, \quad (8)$$

where m_ρ and Γ are the ρ-meson mass and width, respectively.

The two models are compared with the projections of the 3π Dalitz plot for the region $1.0 \leq M(3\pi) \leq 1.1$ GeV, the nominal A_1 region, in Fig. 14. For the Veneziano model, the value $G_s/G_d = -0.15$ GeV^2 gives the best fit to the data (60% confidence level). For the ρ-pole model, the best fit is obtained for this same value of G_s/G_d, but the fit is poorer (3% confidence level).

The results show that the nominal A_1 region of the 3π system is well described by a pure $J^P = 1^+$ amplitude according to either the Veneziano or ρ-pole model. The Veneziano model fits the data notably better than the ρ-pole model, and yields the value $G_s/G_d = -0.15_{-0.15}^{+0.09}$ GeV^2, which is consistent with a theoretical prediction[13] based on the algebraic realization of chiral symmetry.

ACKNOWLEDGMENTS

We wish to thank the personnel of the 30-in. bubble chamber and the ZGS at Argonne National Laboratory for their help and cooperation. We also wish to acknowledge the assistance of J. B. Annable with the data analysis and W. L. Rickhoff and R. Erichsen with the measuring facility. We appreciate the enthusiastic support of the Notre Dame scanning and measuring staff.

[13] F. J. Gilman and H. Harari, Phys. Rev. **165**, 1803 (1968).

PHYSICAL REVIEW D VOLUME 3, NUMBER 3 1 FEBRUARY 1971

Observation of a 7π Enhancement at 3.01 GeV*

G. P. Yost, W. A. Morris, J. R. Albright, E. B. Brucker,† and J. E. Lannutti
Department of Physics, Florida State University, Tallahassee, Florida 32306

(Received 8 September 1970)

In an 11.0-GeV/c π^+p exposure in the BNL 80-in. hydrogen-filled bubble chamber, 171 events have been found that fit the reaction $\pi^+ + p \to 4\pi^+ + 3\pi^- + \pi^0 + p$. The $(4\pi^+3\pi^-)$ and $(3\pi^+3\pi^-\pi^0)$ effective-mass spectra both show a statistically significant peak at 3.013 GeV with a width less than 0.04 GeV. This enhancement agrees well both in position and in width with one of the peaks observed in a CERN missing-mass spectrometer experiment.

RECENTLY it has been reported[1,2] that a number of narrow high-mass boson resonances have been observed in a missing-mass spectrometer (MMS) experiment at CERN. Such objects may have high spins, first because they may be Regge recurrences of lower-lying particles, and second because the narrow widths suggest the operation of angular momentum barrier effects. If this is the case, one may expect them to decay preferentially via other particles with spin, to reduce angular momentum barrier effects. In the case of meson decay modes, this necessarily involves lower-lying resonances, which in turn decay, and so on.[3]

Thus, one might expect to see some of these resonances among multipion final states produced in high-energy collisions in a bubble chamber. One such observation has recently been reported[4] at 3.0 GeV, decaying into six pions, corresponding in position, but not in width, to one of the CERN peaks.[1] The CERN group reports an $X^-(3.02)$ located at 3.025 GeV with a width (full width at half-maximum) of 25 MeV. Alexander *et al.*,[4] report a width of 200 ± 60 MeV. In this article we wish to report the observation of another candidate in the same mass region, decaying into seven pions, and hence of opposite G parity from the effect seen by Alexander *et al.*[4]

The BNL 80-in. bubble chamber was exposed to a π^+ beam of momentum 11.0 GeV/c. Approximately 25 000 pictures were taken, corresponding to about 0.9 μb per event. All reactions with eight charged prongs visible in the chamber were measured. This yielded 171 events fitting the reaction

$$\pi^+ + p \to 4\pi^+ + 3\pi^- + \pi^0 + p \quad (1)$$

after events with a proton with a center-of-mass longitudinal momentum greater than 300 MeV/c in the

* Work supported in part by the U. S. Atomic Energy Commission under Contract No. AT-(40-1)-3509. Computational costs were supported in part by National Science Foundation under Grant No. GJ 367 to the Florida State University Computing Center.

† Present address: Rutgers, The State University, New Brunswick, N. J. 08903.

[1] R. Baud *et al.*, Phys. Letters **31B**, 549 (1970).

[2] For a review of meson resonances, see, e.g., B. Maglić, in *Proceedings of the Lund International Conference on Elementary Particles*, edited by G. von Dardel (Berlingska Boktryckeriet, Lund, Sweden, 1969).

[3] The process of cascade decay processes is known to occur in the case of baryon resonances, and even for lower-lying meson states, such as the A_2.

[4] G. Alexander *et al.*, Phys. Rev. Letters **25**, 63 (1970).